High Resolution Geodetic Measurements of Deformation throughout the Ventura Special Fault Study Area Region

Report for SCEC Award #16171
Submitted March 15, 2017

Investigators: Scott T. Marshall (Appalachian State), Gareth J. Funning (UCR), & Susan E. Owen (JPL)

I. Project Overview

A. Abstract

In the box below, describe the project objectives, methodology, and results obtained and their significance. If this work is a continuation of a multi-year SCEC-funded project, please include major research findings for all previous years in the abstract. (Maximum 250 words.)

Data from the SCEC Ventura Special Fault Study Area have provided new and significantly revised constraints on the subsurface structure of the Ventura-Pitas Point fault system in southern California; however, few data directly constrain fault surfaces below ~6 km depth. Here, we use geometrically complex three-dimensional mechanical models driven by current geodetic strain rates to test two proposed subsurface models of the fault system. We find that the model that incorporates a ramp geometry for the Ventura-Pitas Point fault better reproduces both the regional long term geologic slip rate data and interseismic GPS observations of uplift in the Santa Ynez Mountains. The model-calculated average reverse slip rate for the Ventura-Pitas Point fault is 3.5 ± 0.3 mm/yr, although slip rates are spatially variable on the fault surface with > 8 mm/yr predicted on portions of the lower ramp section at depth. This work effectively accomplishes two of the key goals of the Ventura SFSA: 1) to determine the most likely subsurface fault configuration, and 2) to identify and quantify the interseismic strain associated with the Ventura-Pitas Point fault.

B. SCEC Annual Science Highlights

Each year, the Science Planning Committee reviews and summarizes SCEC research accomplishments, and presents the results to the SCEC community and funding agencies. Rank (in order of preference) the sections in which you would like your project results to appear. Choose up to 3 working groups from below and re-order them according to your preference ranking.

1) Tectonic Geodesy
2) Unified Structural Representation (USR)
3) Stress and Deformation Through Time (SDOT)

C. Exemplary Figure

Select one figure from your project report that best exemplifies the significance of the results. The figure may be used in the SCEC Annual Science Highlights and chosen for the cover of the Annual Meeting Proceedings Volume. In the box below, enter the figure number from the project report, figure caption and figure credits.

Figure 3b-e. b) N20W profile through GPS vertical velocities (gray triangles) in the western Transverse Ranges region. Blue curves show model predictions for the no ramp model. All velocities are relative to station CIRX. c) Cross-sections through the three dimensional model showing the fault geometry at the profile location. Blue horizontal lines show the three locking depths plotted in part a). d-e) Same as b-c) but for the ramp model.

D. SCEC Science Priorities

In the box below, please list (in rank order) the SCEC priorities this project has achieved. See *https://www.scec.org/research/priorities* for list of SCEC research priorities. *For example: 6a, 6b, 6c*

4a, 4b, 4c

E. Intellectual Merit

How does the project contribute to the overall intellectual merit of SCEC? *For example: How does the research contribute to advancing knowledge and understanding in the field and, more specifically, SCEC research objectives? To what extent has the activity developed creative and original concepts?*

This project contributes to the understanding of crustal deformation in southern California by using a novel three-dimensional mechanical modeling approach to simulate both interseismic and long-term deformation. Two primary goals of the Ventura Special Fault Study Area (SFSA) are 1) to determine the most likely fault structure for the region, and 2) to identify and quantify the interseismic deofmration associated with the Ventura-Pitas Point fault. This project has met both of these goals by creating and directly testing the two proposed subsurface fault system geometries for the greater Ventura region using a physics-based method. Our geodetic data processing and analysis has successfully identified the interseismic deformation associated with the Ventura-Pitas Point fault, and furthermore, we have shown that only the ramp model of Hubbard et al. [2014] fits the geodetic data. Our approach offers a quantitative assessment of the ability of the CFM to reproduce variations in slip and interseismic deformation in southern California and demonstrates that the ongoing efforts to revise and improve the SCEC CFM have been very worthwhile. Furthermore, the fault mesh produced in this study has been shared with numerous other SCEC researchers and is included as an electronic supplement in our recent GLR publication.

We hope that the success of this project will facilitate future studies of the slower slipping (but still hazardous) faults in southern California, including the Los Angeles and Ventura basin regions. There are still many facets of this fault system that are poorly studied, especially in the geodetic realm.

F. Broader Impacts

How does the project contribute to the broader impacts of SCEC as a whole? *For example: How well has the activity promoted or supported teaching, training, and learning at your institution or across SCEC? If your project included a SCEC intern, what was his/her contribution? How has your project broadened the participation of underrepresented groups? To what extent has the project enhanced the infrastructure for research and education (e.g., facilities, instrumentation, networks, and partnerships)? What are some possible benefits of the activity to society?*

This work has fostered collaborations between researchers at the Jet Propulsion Laboratory, the University of California Riverside, Harvard University, and Appalachian State University. At Appalachian State University, PI Marshall now routinely trains undergraduate students in GPS/InSAR processing, dislocation modeling, and stress/strain theory. Marshall is currently working with two undergraduate geology students at Appalachian State University on fault modeling and geodesy. One student is modeling the faults of the Imperial Valley region using the CFM, while the other is processing GPS time series to determine seasonal aquifer motions. The student doing the GPS work was a coauthor on our recent GRL publication. These efforts are aimed to produce future researchers that are better prepared for graduate school and the research community. Also, by training undergraduate students, interest and understanding of earthquake science is promoted. The results of this work will have an impact on society by more accurately characterizing the slip rates of faults, which in turn leads to improved seismic hazard estimates.

G. Project Publications

All publications and presentations of the work funded must be entered in the SCEC Publications database. Log in at *http://www.scec.org/user/login* and select the Publications button to enter the SCEC Publications System. Please either (a) update a publication record you previously submitted or (b) add new publication record(s) as needed. If you have any problems, please email *web@scec.org* for assistance.

II. Technical Report

A. Project Objectives

In 2012, SCEC established the Ventura Special Fault Study Area (SFSA) largely based on recent work suggesting the potential for M7.5-8.0 earthquakes in the region [*Hubbard et al.*, 2014; *McAuliffe et al.*, 2015; *Rockwell et al.*, 2016]. Analysis of seismic reflection and borehole data support the presence of a large seismogenic reverse fault structure, the Ventura-Pitas Point (VPP) fault, which has an estimated slip rate of 4.4-6.9 mm/yr. [*Hubbard et al., 2014*; *McAuliffe et al., 2015*]. A reverse fault of this size and slip rate should be detectable with modern geodetic techniques; however, as discussed by *Marshall et al. [2013]*, continuous GPS data in the region are complicated by fast and localized strain rates related to inelastic deformation in the Ventura basin.

The overall objective of this multi-year project is to 1) use geodetic data to detect the interseismic strain signature of the VPP fault and 2) to distinguish which of the two proposed subsurface fault geometries best fits the data. We are pleased to report that we have succeeded in these goals. Based on results from mechanical models, the ramp representation of *Hubbard et al.* [2014] best fits long-term geologic slip rate data, and reproduces GPS measured uplift rates in the Santa Ynez Mountains [*Marshall et al.*, 2017]. We report the details of our results of this multi-year project below.

B. Proposed Models of the Ventura-Pitas Point Fault

Despite numerous analyses of subsurface borehole and geophysical data across the VPP fault [*Sarna-Wojcicki et al.*, 1976; *Yeats*, 1982; 1983; *Rockwell et al.*, 1984; *Huftile and Yeats*, 1995; 1996; *Hubbard et al.*, 2014], few geophysical data exist that can uniquely resolve the VPP fault structure at depths > 6 km. Thus, two distinct models have been proposed for the deep fault structure. The first model, which we term the “ramp model,” is based on *Hubbard et al.* [2014] and represents the VPP fault flattening into a nearly horizontal décollement at ~7 km depth and then steepening into a lower ramp section farther north (Figure 1). The second model, which we term the “no ramp model,” maintains a nearly constant dip angle as is observed in the shallow portions of the fault until the fault merges with the Red Mountain fault at a depth of 10 km. This model is based on extending the near surface portion of the VPP fault to agree with earthquake hypocenters from two recent earthquake aftershock sequences [*Kamerling et al.*, 2003]. These alternate VPP fault geometries are markedly different from past realizations of the fault system [e.g. *Plesch et al.*, 2007; *Marshall et al.*, 2008; *Marshall et al.*, 2013] and imply different structural linkages with several other faults in the region at depth. For example, the ramp model links the VPP and San Cayetano faults at depth whereas the San Cayetano fault is unconnected to any other subsurface structure in the no ramp representation. Furthermore, in the ramp model, the Red Mountain fault is truncated by the VPP fault, so the Red Mountain fault only exists above 8 km depth. Because existing data cannot directly resolve the deep fault structure, both Ventura-Pitas Point fault models are plausible and warrant testing with independent data.

C. Mechanical Modeling Results

The first step in our modeling process is to produce representations of the ensemble fault geometries of the two competing fault geometric models. Our modeled fault surfaces in the western Transverse Ranges are based upon the Southern California Earthquake Center (SCEC) Community Fault Model version 5.0 (CFM5.0), with additional modifications for the ramp and no ramp cases. In total, we model 74 structures in the two alternative fault models, with over 18,000 individual triangular elements in each, and a mean element size of ~3.8 km^2. Next, we use the method of *Marshall et al.* [2013] to estimate the distribution of fault slip on the fault ensembles, testing both the ramp and no ramp cases. This formulation allows us to calculate distributions of fault slip that are kinematically compatible with the applied regional strain rate, while simultaneously accounting for mechanical interactions between all modeled fault elements. In this way, we estimate slip rates for each modeled fault element that can be compared individually or collectively to geologic estimates of long-term slip rates.

The model-calculated average reverse slip rates for each fault, for both the ramp and no ramp cases are compared to existing geologic estimates in Figure 1. For the purposes of comparison, we estimate a single area-weighted average slip rate and area-weighted standard deviation of slip values for each surface and plot the 1σ ranges as error bars in Figure 1. Thus, a large error bar on Figure 1 represents a fault surface with large spatial variations in slip rates. We compare the model calculated average slip rates with two other quantities: 1) geologic reverse slip rate estimates and 2) the corresponding average reverse slip rate estimates from our earlier study [*Marshall et al.*, 2013], based on the older and significantly different CFM4.0 fault geometries which lack structural connections between the VPP faults. Geologic reverse slip rate ranges are taken from the UCERF3 report [*Field et al.*, 2014] with the exceptions of the upper slip bound of 1.4 mm/yr for the Simi fault [*DeVecchio et al.*, 2012], and the 4.4-10.5 mm/yr slip rate range of the VPP [*Hubbard et al.*, 2014]. Although most of the faults in the region are likely to have an oblique component of slip [*Marshall et al.*, 2008], there are no well-constrained long-term estimates of strike-slip rates in the region. We therefore focus on comparing the existing reverse slip rate estimates to the model predictions.

We find that the ramp model agrees with all of the geologic slip rate ranges within the model-calculated 1σ ranges, and that the no ramp model matches fourteen out of fifteen of the geologic slip rates with the only mismatch occurring on the San Cayetano fault. Both of these CFM5.0 models fit the geologic slip rate data better the CFM4.0 model of *Marshall et al.* [2013], which does not fit two key regional faults: the Red Mountain and VPP faults. The CFM4.0 model predicts slower average slip rates on the VPP fault overall than are supported by the geologic data (Figure 1), and due to its small surface area (compared to CFM5.0) is likely incompatible with the numerous recent discoveries of large magnitude uplift events along the fault [*Hubbard et al.*, 2014; *McAuliffe et al.*, 2015; *Rockwell et al.*, 2016].

Due to large uncertainties in the existing long-term slip rate estimates, it is not surprising that all of the models fit the majority of existing slip rates within the existing ranges. To better distinguish which model is most compatible with existing slip rates, we now focus on examples of stark differences in model predicted slip rates between two key regional faults. In the ramp model, the Red Mountain fault is truncated by the VPP fault along the horizontal ramp at a depth of ~7 km, which dramatically slows down the Red Mountain fault slip rates. The no ramp model predicts much faster slip rates for the Red Mountain fault because the VPP fault is truncated by the Red Mountain fault at 10 km depth. In essence, the ramp model geometry suggests that the VPP fault is the master regional fault at depth, and is therefore the main driver of inter-seismic deformation, while the no ramp model suggests the Red Mountain fault is the master fault at depth. We prefer the slower slip rate of the ramp model for the Red Mountain fault because 1) the Red Mountain fault does not have a clear geomorphic signature (i.e. a young sharp topographic scarp), while the VPP does [*McAuliffe et al.*, 2015], and 2) the UCERF3 preferred reverse slip rate is 2 mm/yr [*Field et al.*, 2013], which is only within the 1σ range of the ramp model.

Additionally, the two CFM5.0 models predict significantly different average slip rates for the San Cayetano fault (Figure 1). The ramp model predicts much faster slip rates that are closer to the UCERF3 preferred slip rate of 6 mm/yr for the San Cayetano fault. We therefore again suggest that the ramp model better fits the geologic slip rate data.

Long term fault slip rates throughout the western Transverse Ranges are likely to exhibit significant spatial variations [e.g. *Marshall et al.*, 2008]. Given that the long term slip rate estimate of *Hubbard et al.* [2014] is based on data that spans only small portion of the VPP fault surface, we now seek to determine which model predicts compatible slip rates at the location of the existing estimate, and if the existing estimate was made in a location that should yield an average value for the entire fault surface. To accomplish this, we compute the distribution of slip rates at the surface of the modeled half-space, which simulates the slip that may be observed in the near surface by a geologic or near-surface geophysical study.

At the location of the *Hubbard et al.* [2014] study, both models predict local reverse slip rates that are compatible with the long term slip rate estimate within the error limits (Figure 2). Additionally, the ramp model predicts slip rates on the lower ramp section that exceed 8 mm/yr in some locations, which is compatible with the *Hubbard et al.* [2014] deep slip rate of 6.6-10.5 mm/yr.

The *Hubbard et al.* [2014] slip rate estimate for the VPP fault is located near the middle of the VPP fault trace where both the ramp and no ramp models predict slip rates that are faster than the weighted average slip rate over the entire VPP fault surface (Figure 2). In fact, both models predict the fastest near

surface slip rates should occur near the location of the *Hubbard et al.* [2014] study. According to the ramp and no ramp models, the location of the *Hubbard et al.* [2014] slip rate estimate should yield reverse slip rates that are 15% and 79%, respectively, above average for the VPP fault as a whole.

D. GPS Processing and Interseismic Modeling

An alternative means of testing the competing VPP models against data is to simulate the expected interseismic deformation rates for each and compare them to GPS data. Since the ramp and no ramp representations use significantly different deep fault structures for the VPP and Red Mountain faults, the interseismic deformation produced by these two models is distinct.

For this analysis, we use continuous GPS data from 56 stations in the Plate Boundary Observatory (PBO) network provided by the MEaSUREs, although we note that during this project we processed a total of 347 total GPS stations throughout southern California. Here, we use the minimally pre-processed daily 'raw-trended' time series data, and apply an established time series processing methodology [*Marshall et al.*, 2013; *Herbert et al.*, 2014], which we summarize here.

We select GPS stations with more than two years of data since 2004, which postdates the vast majority of postseismic transient motion associated with the 1999 M7.1 Hector Mine earthquake [*Shen et al.*, 2011]. To estimate secular velocities at each station, we estimate and remove annual and semi-annual motions, offsets from equipment changes, common mode error [*Dong et al.*, 2006], and co- and post-seismic deformation associated with the 2010 M7.2 El Mayor Cucapah earthquake [*Gonzalez-Ortega et al.*, 2014]. To isolate the tectonic deformation associated with only faults in the western Transverse Ranges region, we additionally remove interseismic deformation associated with the San Andreas, San Jacinto, and Garlock faults using a kinematic rectangular dislocation model using the geometry, fault slip rates, and locking depths from *Loveless and Meade* [2011]. We discard two GPS sites in the western Transverse Ranges region due to clearly anomalous vertical velocities: VNCO and P729. Both of these sites were identified by *Marshall et al.* [2013] as being in a zone of subsidence due to groundwater extraction.

Existing studies of GPS velocities from the western Transverse Ranges region all show a highly localized horizontal velocity gradient located directly above the Ventura sedimentary basin [*Donnellan et al.*, 1993a; 1993b; *Hager et al.*, 1999; *Marshall et al.*, 2013]. *Hager et al.* [1999] showed that this sharp contraction gradient could be reproduced with a two-dimensional finite element model with a spatially-variable low elastic modulus feature simulating the Ventura sedimentary basin. As a result, *Marshall et al.* [2013] argue that the horizontal GPS velocities in the western Transverse Ranges region are likely significantly contaminated by non-faulting-related deformation processes acting in the Ventura sedimentary basin. Therefore, we focus here on whether the ramp or no ramp models better fit the vertical GPS deformation patterns.

In order to simulate interseismic deformation, we create a second set of models where we prescribe the geologic timescale model-calculated slip rate values on elements below a chosen locking depth and lock all elements above that depth [*Marshall et al.*, 2009]. These interseismic forward models can then be used to predict the velocities at the locations of GPS stations. We note that these interseismic models are forward models, and therefore may not fit the GPS data as well as a typical inverse model; however, since the interseismic models used here are based on the mechanical model calculated slip rates, we can be certain that the subsurface slip rate distributions are mechanically plausible. The focus here is to determine only which model fits the general patterns of vertical deformation in the region.

Since the GPS data are spatially sparse (Figure 3a), we project the vertical velocities of reliable sites within a 40km wide zone onto a N20W profile that extends through the western Transverse Ranges region (Figure 5). In general, the GPS profile shows ~1 mm/yr of subsidence across the Ventura basin (approximately 25-55 km distance on Figure 3b-e) and ~1 mm/yr of uplift to the north of the basin (60-80 km on Figure 3b-e). Interseismic model predictions for locking depths of 10, 15, and 20 km clearly show that the no ramp model produces uplift too far south compared to the GPS data. On the other hand, the ramp model with a locking depth of 15 km predicts loci of relative uplift and subsidence in the approximately correct locations and therefore fits the general pattern of GPS vertical deformation well overall. The under-fitting of the subsidence signal (e.g. 30–55 km in Figure 5) is likely due to nontectonic compaction in the sediments

of the Ventura basin [e.g. *Nicholson et al.*, 2007]. Therefore, we argue, that the vertical GPS data clearly favor a model that includes a shallow crustal ramp.

E. InSAR Processing

To date, we have processed Envisat InSAR data that span 2005-2010 (24 scenes) and ERS InSAR Data that span 1995-2000 (29 total scenes). A significant portion of the western Transverse Ranges is vegetated and/or contains steep topographic slopes, therefore backscattered radiation from c-band radar satellites imaging the region severely decorrelates with time [*Zebker and Villasenor, 1992*; *Hooper et al., 2004*], rendering traditional, '2-pass' InSAR methods ineffective. These problems are mitigated to a large degree by applying an advanced processing methodology to InSAR data for the region to identify 'persistent scatterers' – targets on the ground that provide radar returns that are stable throughout time. Using the Stanford Method for Persistent Scatterers (StaMPS) technique of *Hooper et al.* [*2004*; *2008*], we have calculated line of sight (LOS) velocities for several million persistent scatterer pixels on the ground for the ERS and Envisat data. Unfortunately, the dominant signals observed in both datasets are related to hydrocarbon and groundwater extraction near the Central Valley, groundwater withdrawal near the cities of Oxnard and Ventura, and numerous atmospheric-related signals (i.e. noise). The region of interseismic uplift related to the VPP fault lies in the vegetated and steep-sloped Santa Ynez mountains (Figure 3a), where both InSAR datasets yield sparse persistent scatterers and noisy data. The InSAR data was useful for identifying which GPS sites are recording non-tectonic motions, but unfortunately, the InSAR data in the Sanat Ynez mountains was unreliable and not directly useful for comparing to model results. With newer L-Band InSAR data and improving atmospheric correction models, future efforts may be able to use InSAR to better delineate the VPP fault interseismic deformation. Fortunately, we were successful at identifying the interseismic VPP fault strain with the most recent PBO GPS data.

F. Conclusions

The CFM5.0 represents a significant update compared to previous CFM versions with completely updated representations of the VPP and several other major regional faults. Based on mechanical model results, CFM5.0 based mechanical models better match long term geologic slip rates compared to CFM4.0 based models. This is a clear indication that the continuing SCEC efforts to update and refine the CFM are worthwhile and valuable. With this improved deformation model, we have now published updated model-calculated slip rate estimates for all of the regional faults within the region where our modeled boundary conditions are appropriate [*Marshall et al.*, 2017].

Uncertainty in the deep geometry of the VPP fault has led to the proposal of two distinct subsurface models (with and without a midcrustal ramp structure) in the CFM5.0. Mechanical model predictions indicate that the ramp model of the VPP fault is more compatible with existing regional geologic slip rate data compared to the no ramp model because the no ramp model predicts geologically unlikely slip rates along the Red Mountain and San Cayetano faults. Comparisons of CFM5.0 interseismic models to vertical GPS velocities show that the no ramp model predicts interseismic uplift ~15 km too far south compared to the GPS velocities. In contrast, the ramp model predicts loci of uplift and subsidence that largely agree with the data. In the end, mechanical model predictions favor a ramp geometry for the VPP fault.

G. References

DeVecchio, D. E., E. A. Keller, M. Fuchs, and L. A. Owen (2012), Late Pleistocene structural evolution of the Camarillo fold belt: Implications for lateral fault growth and seismic hazard in Southern California, *Lithosphere*, *4*(2), 91-109, doi:10.1130/l136.1.

Dong, D., P. Fang, Y. Bock, F. H. Webb, L. Prawirodirdjo, S. Kedar, and P. Jamason (2006), Spatiotemporal filtering using principal component analysis and Karhunen-Loeve expansion approaches for regional GPS network analysis, *Journal of Geophysical Research*, *111*(B03405), doi:10.1029/2005JB003806.

Donnellan, A., B. H. Hager, and R. W. King (1993a), Discrepancy between geological and geodetic deformation rates in the Ventura Basin, *Nature*, *366*(6453), 333-336, doi:10.1029/93JB02766.

Donnellan, A., B. H. Hager, R. W. King, and T. A. Herring (1993b), Geodetic measurement of deformation in the Ventura Basin region, Southern California, *Journal of Geophysical Research*, *98*(B12), 727-721.

Field, E. H., et al. (2014), Uniform California Earthquake Rupture Forecast, Version 3 (UCERF3)—The Time-Independent Model, *Bulletin of the Seismological Society of America*, *104*(3), 1122-1180, doi:10.1785/0120130164.

Field, E. H., et al. (2013), Uniform California earthquake rupture forecast, version 3 (UCERF3) - The time-independent model: *Rep.*

Gonzalez-Ortega, A., Y. Fialko, D. Sandwell, A. F. N.-P., J. Fletcher, J. Gonzalez-Garcia, B. Lipovsky, M. Floyd, and G. J. Funning (2014), El Mayor-Cucapah (Mw 7.2) earthquake: Early near-field postseismic deformation from InSAR and GPS observations, *Journal of Geophysical Research: Solid Earth*, *119*(2), 1482-1497, doi:10.1002/2013JB010193.

Hager, B. H., G. A. Lyzenga, A. Donnellan, and D. Dong (1999), Reconciling rapid strain accumulation with deep seismogenic fault planes in the Ventura Basin, California, *Journal of Geophysical Research*, *104*(B11), 25,207-225,219.

Herbert, J. W., M. L. Cooke, and S. T. Marshall (2014), Influence of fault connectivity on slip rates in southern California: Potential impact on discrepancies between geodetic derived and geologic slip rates, *Journal of Geophysical Research: Solid Earth*, *119*(3), 2342-2361, doi:10.1002/2013JB010472.

Hooper, A. (2008), A multi-temporal InSAR method incorporating both persistent scatterer and small baseline approaches, *Geophysical Research Letters*, *35*(L16302), doi:10.1029/2008GL034654.

Hooper, A., H. Zebker, P. Segall, and B. Kampes (2004), A new method for measuring deformation on volcanoes and other natural terrains using InSAR persistent scatterers, *Geophysical Research Letters*, *31*(23), doi:10.1029/2004GL021737.

Hubbard, J., J. H. Shaw, J. F. Dolan, T. L. Pratt, L. McAuliffe, and T. K. Rockwell (2014), Structure and seismic hazard of the Ventura Avenue anticline and Ventura fault, California: Prospect for large, multisegment ruptures in the Western Transverse Ranges, *Bulletin of the Seismological Society of America*, *104*(3), 1070-1087, doi:10.1785/0120130125.

Huftile, G. J., and R. S. Yeats (1995), Convergence rates across a displacement transfer zone in the western Transverse Ranges, Ventura Basin, California, *Journal of Geophysical Research*, *100*(B2), 2043-2067.

Huftile, G. J., and R. S. Yeats (1996), Deformation rates across the Placerita (Northridge M (sub w) = 6 7 aftershock zone) and Hopper Canyon segments of the western Transverse Ranges deformation belt, *Bulletin of the Seismological Society of America*, *86*(1), 3-18.

Kamerling, M., C. C. Sorlien, and C. Nicholson (2003), 3D development of an active, oblique fault system, northern Santa Barbara Channel, CA, in *Seismological Society of America Annual Meeting with Abstracts*, edited.

Loveless, J. P., and B. J. Meade (2011), Stress modulation on the San Andreas fault by interseismic fault system interactions, *Geology*, *39*(11), 1035-1038, doi:10.1130/g32215.1.

Marshall, S. T., M. L. Cooke, and S. E. Owen (2008), Effects of non-planar fault topology and mechanical interaction on fault slip distributions in the Ventura Basin, California, *Bulletin of the Seismological Society of America*, *98*(3), 1113-1127, doi:10.1785/0120070159.

Marshall, S. T., M. L. Cooke, and S. E. Owen (2009), Interseismic deformation associated with three-dimensional faults in the greater Los Angeles region, California, *Journal of Geophysical Research*, *114*(B12403), 1-17, doi:10.1029/2009JB006439.

Marshall, S. T., G. J. Funning, H. E. Krueger, S. E. Owen, and J. P. Loveless (2017), Mechanical models favor a ramp geometry for the Ventura-pitas point fault, California, *Geophysical Research Letters*, *44*(3), 1311-1319, doi:10.1002/2016GL072289.

Marshall, S. T., G. J. Funning, and S. E. Owen (2013), Fault slip rates and interseismic deformation in the western Transverse Ranges, CA, *Journal of Geophysical Research*, *118*, 4511-4534, doi:10.1002/jgrb.50312.

McAuliffe, L. J., J. F. Dolan, E. J. Rhodes, J. Hubbard, J. H. Shaw, and T. L. Pratt (2015), Paleoseismologic evidence for large-magnitude (Mw 7.5–8.0) earthquakes on the Ventura blind thrust fault: Implications for multifault ruptures in the Transverse Ranges of southern California, *Geosphere*, *11*(5), 1629-1650, doi:10.1130/ges01123.1.

Nicholson, C., M. J. Kamerling, C. C. Sorlien, T. E. Hopps, and J.-P. Gratier (2007), Subsidence, Compaction, and Gravity Sliding: Implications for 3D Geometry, Dynamic Rupture, and Seismic Hazard of Active Basin- Bounding Faults in Southern California, *Bulletin of the Seismological Society of America*, *97*(5), 1607-1620, doi:10.1785/0120060236.

Plesch, A., et al. (2007), Community Fault Model (CFM) for Southern California, *Bulletin of the Seismological Society of America*, *97*, 1793-1802.

Rockwell, T. K., K. Clark, L. Gamble, M. Oskin, E. C. Haaker, and G. L. Kennedy (2016), Large Transverse Ranges earthquakes cause coastal upheaval near Ventura, southern California, *Bulletin of the Seismological Society of America*, *106*(6), doi:10.1785/0120150378.

Rockwell, T. K., E. A. Keller, M. N. Clark, and D. L. Johnson (1984), Chronology and rates of faulting of Ventura River terraces, California, *Geological Society of America Bulletin*, *95*, 1466-1474.

Sarna-Wojcicki, A. M., K. M. Williams, and R. F. Yerkes (1976), Geology of the Ventura fault, Ventura County, California, U.S. Geological Survey.

Shen, Z. K., R. W. King, D. C. Agnew, M. Wang, T. A. Herring, D. Dong, and P. Fang (2011), A unified analysis of crustal motion in Southern California, 1970–2004: The SCEC crustal motion map, *Journal of Geophysical Research: Solid Earth*, *116*(B11), B11402, doi:10.1029/2011JB008549.

Yeats, R. S. (1982), Low-shake faults of the Ventura basin, California, in *Neotectonics in Southern California*, edited by J. D. Cooper, pp. 3-15, Geological Society of America.

Yeats, R. S. (1983), Large-scale Quaternary detachments in Ventura Basin, southern California, *Journal of Geophysical Research*, *88*(B1), 569-583, doi:10.1029/JB088iB01p00569.

Zebker, H., and J. Villasenor (1992), Decorrelation in interferometric radar echoes, *IEEE Transactions on Geoscience and Remote Sensing*, *30*(5), 950-959, doi:10.1109/36.175330.

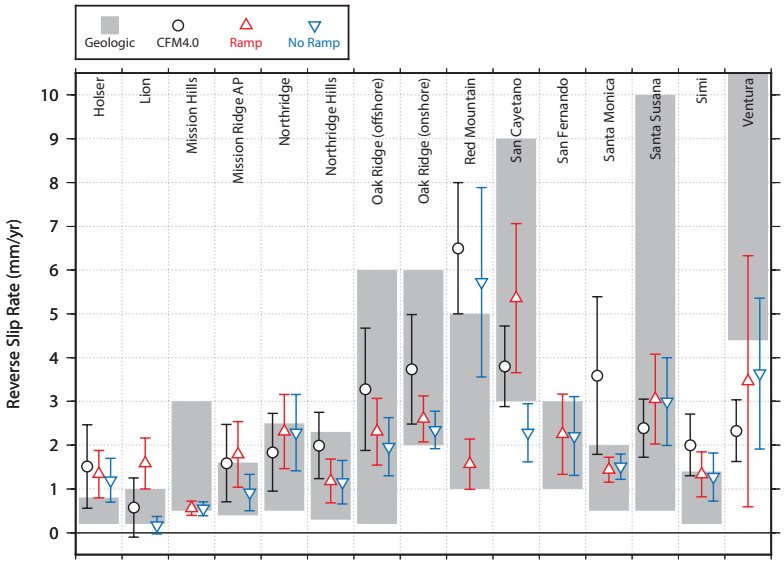

Figure 1. Model-calculated area-weighted average reverse slip rates (symbols) compared to existing geologic slip rate estimates (gray rectangles) for faults in the western Transverse Ranges region. For model-calculations, only elements within the seismogenic crust (< 20 km depth) are used in the calculation.

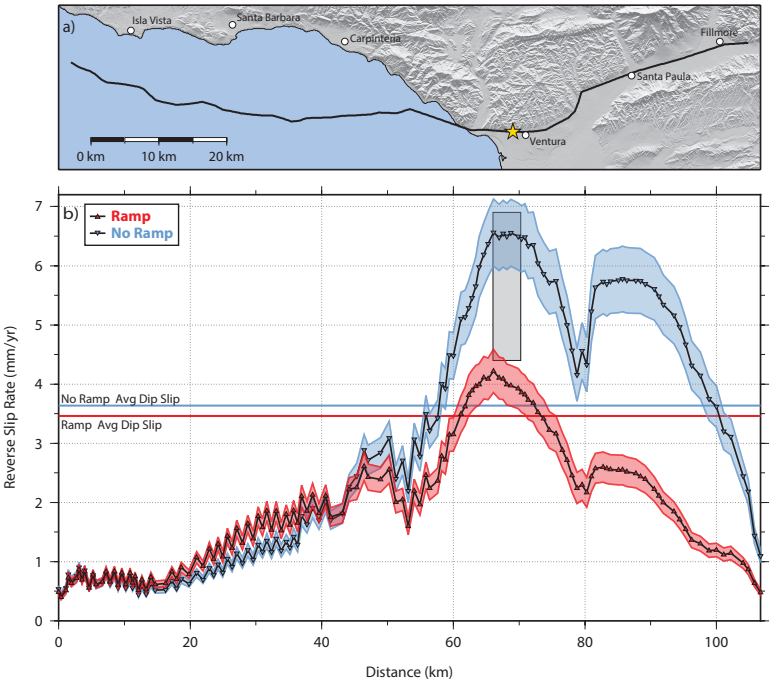

Figure 2. a) Fault trace map of the VPP fault. A gold star marks the location of the slip rate estimate of Hubbard et al. [2014]. b) Model-predicted slip distributions at the surface of the Earth for the VPP fault. The gray rectangle shows the location and reverse slip rate range estimated by Hubbard et al. [2014]. The red and blue ranges reflect uncertainty in the regional strain rate boundary conditions.

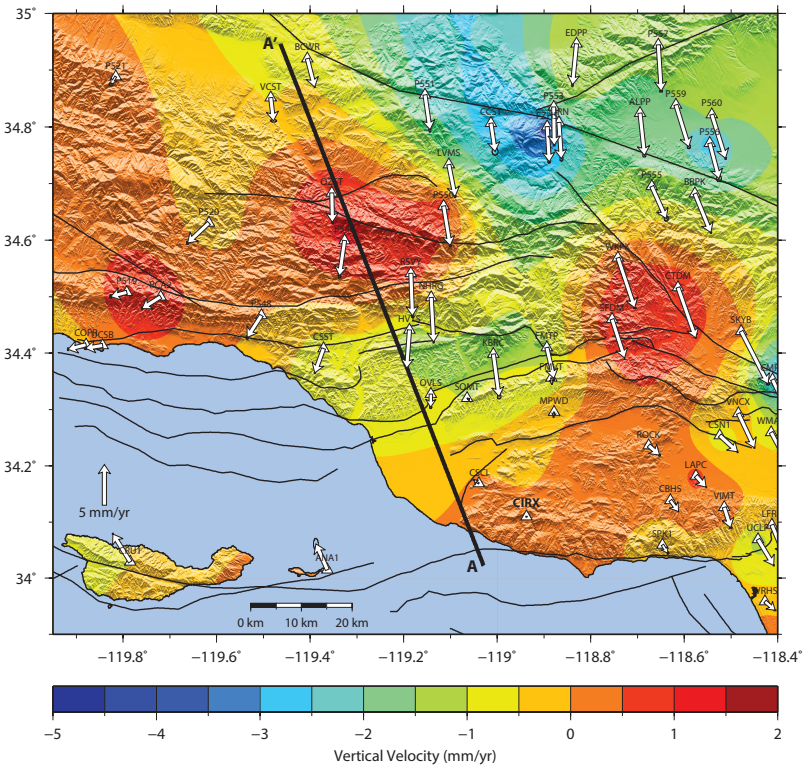

Figure 3a. GPS horizontal (arrows) and vertical (colored contours) velocities relative to station CIRX in the Santa Monica Mountains. Thick black lines indicate the location of profiles used in Figure 1 (A-A') and Figure 5 (B-B'). Stations AOA1, TOST, VNCO, P729, CUHS, BKR1, TABV, and P554 are excluded here due to clearly anomalous vertical velocities.

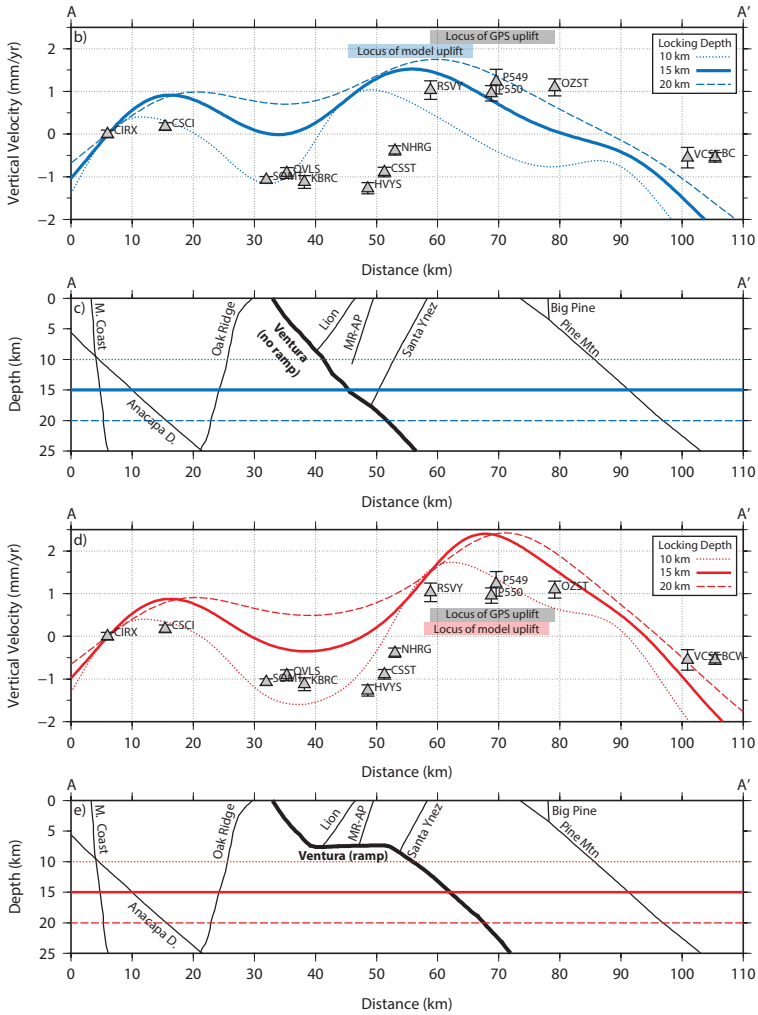

Figure 3b-e. b) N20W profile through GPS vertical velocities (gray triangles) in the western Transverse Ranges region. Blue curves show model predictions for the no ramp model. All velocities are relative to station CIRX. c) Cross-sections through the three dimensional model showing the fault geometry at the profile location. Blue horizontal lines show the three locking depths plotted in part a). d-e) Same as b-c) but for the ramp model.